

Development of anomalous x-ray scattering for partial structure studies of random systems¹⁾

Shinya HOSOKAWA^{1,2} and Jens Rüdiger STELLHORN^{1,2}

¹⁾ *Department of Physics, Kumamoto University, Kumamoto 860-8555, Japan*

²⁾ *Department of Chemistry, Physical Chemistry, Philipps University of Marburg, 35032 Marburg, Germany*

(Received March 8, 2017)

Recent developments of the anomalous x-ray scattering (AXS) measurements for the partial structure characterizations are reviewed. The use of AXS data in combination with reverse Monte Carlo (RMC) modeling highly improves the quality of the partial structural information. A typical example on amorphous phase change materials $(\text{GeTe})_{1-x}(\text{Sb}_2\text{Te}_3)_x$ is introduced to show the feasibility of the AXS and RMC techniques.

§1. Introduction

For the structural studies of non-crystalline multi-component materials, the heaviest task for experimental researchers is to obtain partial information from diffraction experiments. The total structure factors, $S(Q)$, of n -component alloys can be expressed by a linear combination of the Faber-Ziman-type partial structure factors, $S_{ij}(Q)$, as

$$S(Q) = \sum_{i=1}^n \sum_{j=1}^n W_{ij} S_{ij}(Q) \quad (1.1)$$

where the weighting factors, W_{ij} , are given by

$$W_{ij} = x_i x_j \frac{f_i^* f_j}{\langle f \rangle^2} \quad (1.2)$$

Here, x_i is the concentration and f_i is the atomic form factor for x-rays or the atomic scattering length for neutrons, of the i -th element. The chemical average is represented by $\langle \rangle$. Thus, the number of the partial correlations, $n(n-1)/2$, dramatically increases with increasing n . Thus, a number of scattering experiments with different f values are necessary to obtain the complete sets of the partial correlation functions.

One of the strongest tools to solve this difficulty is neutron diffraction with isotopic substitution (NDIS).²⁾ Since the contrasts between the scattering lengths of isotopes are generally very large, this technique provides very reliable partial information. However, suitable isotopes are very limited and costly. Moreover, the sample must be replaced for each scattering experiment, and there is no guarantee that all the samples have the same atomic structure since microscopic glassy structure highly depends on the thermal history.

Another useful experimental method reviewed in this article is anomalous x-ray

scattering (AXS) technique.³⁾ AXS utilizes the anomalous variation of f for a specific element if the incident x-ray energy is close to its absorption edge. The complex f function is given as

$$f(Q, E) = f_0(Q) + f'(E) + if''(E) \quad (1.3)$$

where f_0 is the usual energy-independent term, and f' and f'' are the real and imaginary parts of the anomalous term, respectively. In general, f is determined by the Q -dependent f_0 in a normal x-ray scattering process, and the anomalous terms are negligible. When the incident x-ray energy approaches an absorption edge of one of the constituent elements, however, the energy-dependent f' and f'' become important. f' has a large negative minimum and f'' shows an abrupt jump near the corresponding absorption edge energy, causing a change in $S(Q)$. In contrast to the NDIS technique, AXS uses only one sample through all of the experiments by only changing the incident x-ray energy, i.e., costly isotopes are not necessary and the sample has the same thermal history.

In this article, we review the recent progress of AXS technique^{4),5)} carried out at ESRF and SPring-8, and show a typical example on amorphous phase change materials $(\text{GeTe})_{1-x}(\text{Sb}_2\text{Te}_3)_x$.⁶⁾⁻⁸⁾

§2. Details of anomalous x-ray scattering

Figure 1 shows the energy dependence of the theoretical f' and f'' values of Sb (dashed curves) and Te (solid curves). The jumps in f'' indicate the absorption edge of each element. As seen in the figure, f' remarkably decreases near the absorption edge energy of each element. Thus, the scattering intensity concerning the edge element decreases with approaching the edge. If two x-ray scattering experiments are carried out at energies far from and very close to an edge of the k -th element as shown by arrows in the figure, the difference of the scattering intensities, or differential structure factor, $\Delta_k S(Q)$, highly enhances the contributions of the k -th element-related partials and suppress the others. $\Delta_k S(Q)$ can also be expressed by a linear combination of $S_{ij}(Q)$ and the f terms of W_{ij} in Eq. (1.2) are replaced by $\Delta_k[\]$, indicating the difference of values in the bracket at the two incident x-ray energies near the absorption edge of the k -th element.

Since the contrast produced by the anomalous terms in f is typically some % of the total scattering intensity, several technical improvements were necessary to obtain the scattering data with a good statistical quality. As reviewed in ref. 5) in detail, the use of intense third-generation synchrotron radiation (SR) did not effectively help to improve the statistics, and the crucial problem was that no suitable detecting system could be prepared for scattered x-rays. The tasks for that are mainly threefold:

1. Typical solid state detectors (SSD) used for the previous AXS experiments³⁾ have a blind time of about 1 μs , and thus the linear response of the detector is lost over a count rate of 20,000 cps. Note that this value is not only the elastic signals, but the total counts of incoming x-rays including several fluorescent and Compton scattering x-rays.

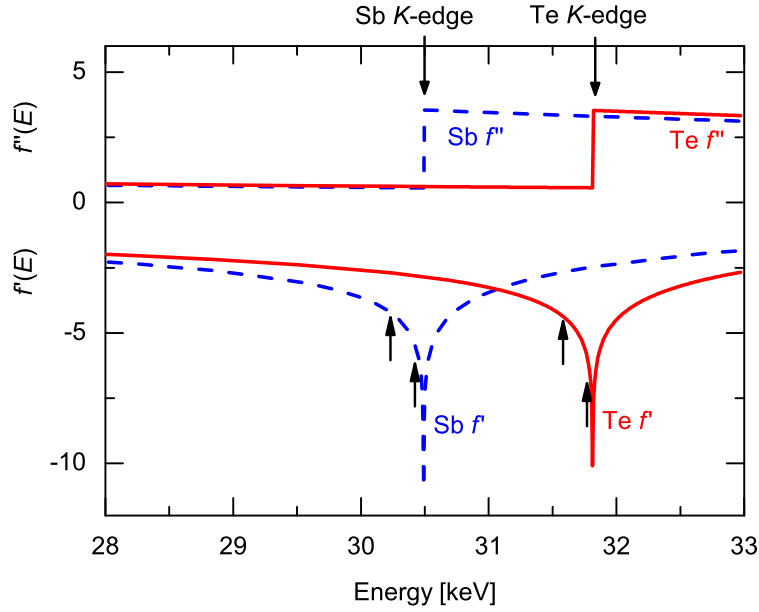


Fig. 1. f' and f'' of Sb (dashed curves) and Te (solid curves). Upward arrows indicate the energies where scattering experiments were performed.

2. A moderate energy resolution of more than 150 eV of the SSD cannot discriminate elastic signals from fluorescent and Compton scattering x-rays, and complex analyses are essential to evaluate $S(Q)$.
3. At least several days are necessary to evaluate $\Delta_k S(Q)$, and the data quality cannot be judged within a limited beamtime for AXS experiments.

To overcome the above difficulties of the detecting system, a new system was developed, the details of which are published elsewhere.^{5),9)} Figure 2 shows a schematic diagram of the new detecting system. The system is mainly composed of a usual NaI scintillation counter with a blind time of about 10 ns and a sagittally bent graphite crystal energy analyzer.

The bent crystals were manufactured with three different curvatures of the radius 90 mm for low x-ray energies of 9-13 keV (typically near the Ge, As, and Se K edges), 60 mm for medium energies of 15-25 keV (near the Ag K edge), and 21 mm for high energies of 30-35 keV (near the Sb and Te K edges). The sagittal form of the bent crystals can focus the vertically scattered x-rays to the detector, increasing the detected intensities by a factor of 3-4, and allows the energy changes of several keV.

By using a long detector arm of about 1 m and an adequate horizontal slits, a good energy resolution of about 60 eV was obtained near the Ge K edge, which can well discriminate the elastic signals from inelastic ones such as fluorescent and Compton scattering. Regarding the counting rate, more than four million counts could be collected at the $S(Q)$ maximum, which typically took 3-5 h per scan.

Since the obtained scattering data are mostly elastic signals, the typical duration of the data analysis is only about 1 h until obtaining a preliminary $\Delta_k S(Q)$ result, and we can immediately judge if the experiment was successful just after the

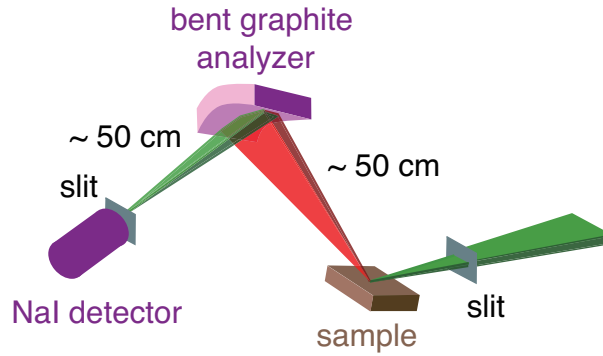


Fig. 2. Schematic diagram of the new detecting system.

experiment.

The use of a fast two-dimensional (2D) detector is one of the recent further improvements in the detecting system, which enable the further increase of the counting rate by a factor of 2-3, and more importantly suppress the experimental errors in the Q dependence of $S(Q)$ or $\Delta_k S(Q)$ owing to the mis-alignments of the positions of the analyzer crystal and the sample with respect to the goniometer.

§3. Reverse Monte Carlo modeling

Reverse Monte Carlo (RMC) modeling¹⁰⁾ is a useful tool to construct 3D structural models of disordered materials using only experimental diffraction data. In the RMC simulation, atoms of initial configuration are moved so as to minimize the deviation from the diffraction data, e.g., $S(Q)$ and $\Delta_k S(Q)$'s, by a standard Metropolis Monte Carlo algorithm.¹¹⁾

Usually a random configuration or a result of a hard-sphere Monte Carlo simulation containing typically 5,000-10,000 atoms was used as a starting configuration. Some constraints such as shortest interatomic distances were applied to the RMC processes to avoid any physically unreliable structures. The RMC calculations were then performed using the RMC++ or RMC_POT program package coded by Gereben et al.¹²⁾ with differently weighted diffraction data. A simulating box size was chosen to match the number densities of the samples.

§4. Examples

We have so far carried out AXS experiments on a number of semiconducting and metallic glasses, and the results were successfully analyzed using the RMC calculation (see refs. 4), 5) and references therein). In this article, we introduce the results of amorphous phase of $(\text{GeTe})_{1-x}(\text{Sb}_2\text{Te}_3)_x$ phase change materials as a typical example.

Rewritable optical storage devices like DVD or blu-ray have meanwhile become common media for data storage, and are used in all areas of daily life. The writing/erasing process in these devices is attained by a reversible laser-induced

crystalline-amorphous transition of the so-called phase change materials such as $(\text{GeTe})_{1-x}(\text{Sb}_2\text{Te}_3)_x$. The transition occurs on a time scale of a several ten ns,¹³⁾ and is accompanied by a significant change in the optical and electrical properties. On the other hand, both the phases should be sufficiently stable for more than ten years at ambient conditions. The important step toward an understanding of the phase change mechanism is a detailed knowledge of the atomistic structure participating on the phase transition.

To investigate the local- and intermediate-range order in amorphous $\text{Ge}_2\text{Sb}_2\text{Te}_5$ ($x = 1/3$) alloy, AXS experiments were carried out at energies close to the Ge, Sb, and Te K edges.^{6)–8)} The circles in Fig. 3 show $\Delta_k S(Q)$'s close to the Ge (red), Sb (purple), and Te (blue) K edges, together with $S(Q)$ (black) measured at 300 eV below the Te K edge. The solid curves represent the best fits of the RMC modeling, which coincide well with the experimental data.

These functions already indicate some interesting features. $\Delta_{\text{Sb}}S(Q)$ and $\Delta_{\text{Te}}S(Q)$ show very similar features to $S(Q)$. In $\Delta_{\text{Ge}}S(Q)$, on the other hand, a prominent first sharp diffraction peak (FSDP) is observed at $Q \sim 10 \text{ nm}^{-1}$, indicating the existence of an intermediate-range atomic correlation concerning the Ge atoms. Also,

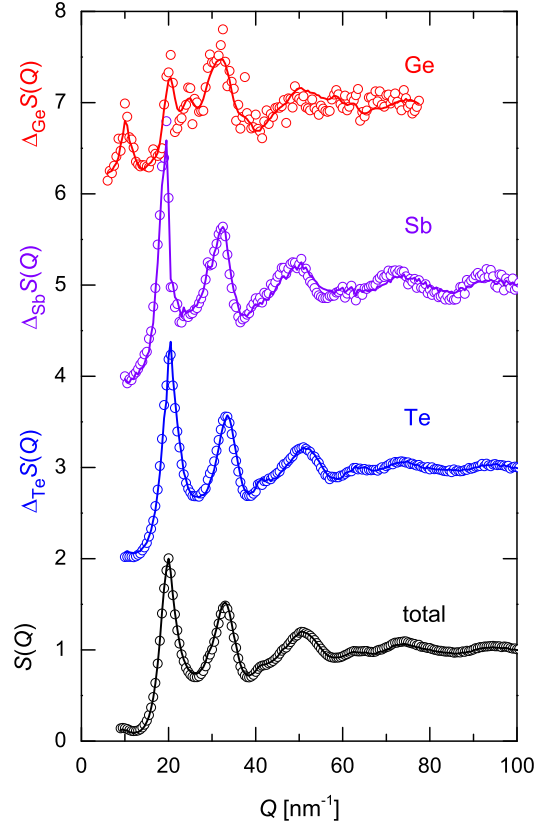


Fig. 3. Circles show $\Delta_k S(Q)$'s close to the Ge (red), Sb (purple), and Te (blue) K edges, together with $S(Q)$ (black). Solid curves represent the best fits of the RMC modeling.

$\Delta_{\text{Ge}}S(Q)$ shows only a small contribution to the main peak at $Q \sim 20 \text{ nm}^{-1}$. Thus, there is no doubt that the atomic arrangements around the Ge atoms are considerably different from the sites of the other constituents in the amorphous phase.

Figure 4 shows (a) $S_{ij}(Q)$'s and (b) $g_{ij}(r)$'s of $\text{Ge}_2\text{Sb}_2\text{Te}_5$ obtained from the RMC modeling for the AXS data. Concerning the FSDP at $Q \sim 10 \text{ nm}^{-1}$ in $S_{ij}(Q)$'s, the Ge-Ge partial shows the most prominent peak. The Ge-Te partial exhibits a smaller contribution. This is another indication for an intermediate-range order on the basis of a Ge-Te network, which seems to play an important role. The Sb-Te partial correlation resembles $S(Q)$ shown in the bottom of Fig. 3, and mostly no FSDP is observed.

The $g_{ij}(r)$ functions obtained from AXS indicate the first coordination shell for all partial correlations in the range between 0.25 and 0.31 nm. Total coordination numbers around each element can be calculated by the integral over the first coordination shell. It is found that Ge and Sb are slightly undercoordinated with respect to the coordination expected from the $8 - N$ rule. On the other hand, Te

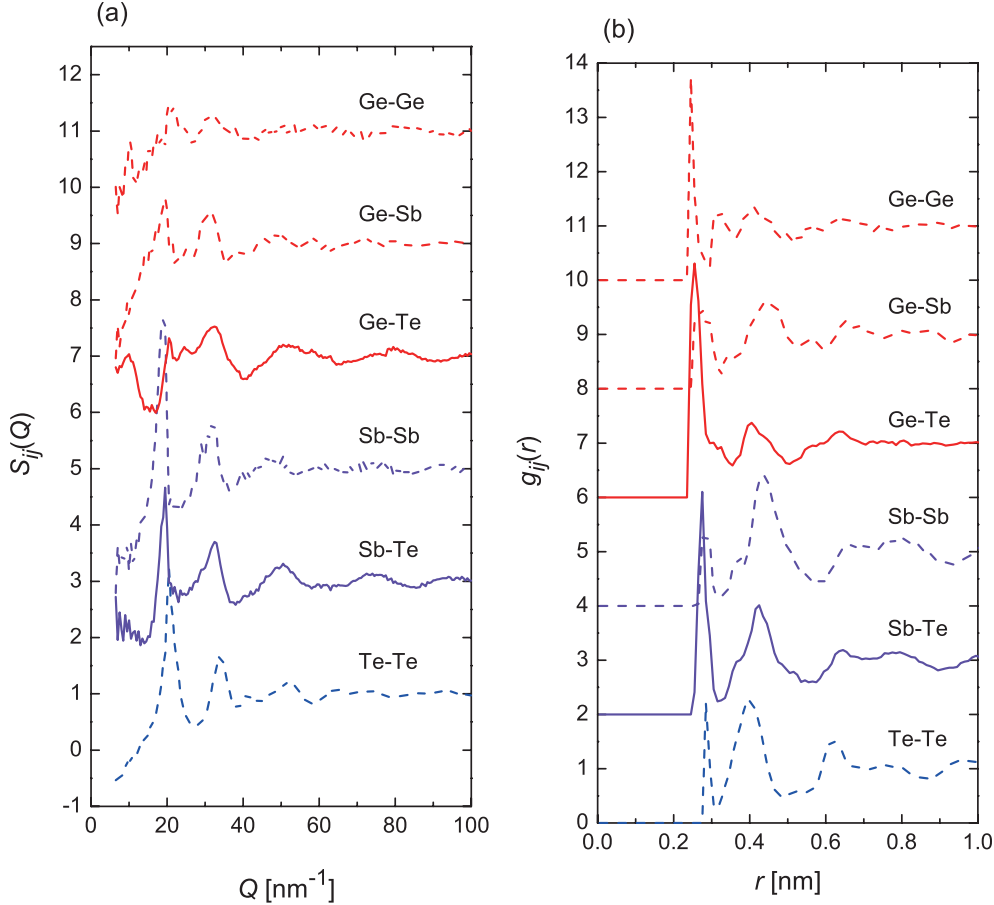


Fig. 4. (a) $S_{ij}(Q)$'s and (b) $g_{ij}(r)$'s of $\text{Ge}_2\text{Sb}_2\text{Te}_5$ obtained from the RMC modeling for the AXS data.

is highly overcoordinated with a coordination number of 2.6. There are significant contributions from homopolar bonds, especially for Te with a partial coordination number of $n_{\text{TeTe}} = 0.77$. For the partial correlations in general, the most intense peaks are found for the Ge-Te and Sb-Te partials. The partial coordination numbers are $n_{\text{GeTe}} = 2.71$ and $n_{\text{SbTe}} = 1.96$, with the peak maxima located at $r_{\text{GeTe}} = 0.26$ nm and $r_{\text{SbTe}} = 0.275$ nm, respectively. Typical building blocks in $\text{Ge}_2\text{Sb}_2\text{Te}_5$ are, thus, SbTe_3 tetrahedra around Ge and distorted pyramidal GeTe_2 blocks around Sb.

§5. Summary

We have developed a new detecting system for AXS, which could fully utilize intense x-ray fluxes from third-generation synchrotron radiation facilities, and solved several difficult issues for the structural characterizations on multi-component non-crystalline materials, such as a good energy resolution, a sufficient counting rate during a limited beamtime, and a time-consuming data analysis. $\Delta_k S(Q)$ functions obtained from AXS were analyzed using RMC modeling to draw 3D atomic configurations. We introduce the results of $\text{Ge}_2\text{Sb}_2\text{Te}_5$ phase change material, and describe its structure-property relation.

We hope that AXS in combination with RMC modeling is capable to become a standard method for investigating local- and intermediate-range atomic structures. Moreover, time-resolved AXS measurements for e.g., phase change materials can be realized in the near future using more intense flux from an undulator device and a faster x-ray detector.

Acknowledgments

The AXS experiments were performed in collaboration with Prof. W.-C. Pilgrim, Prof. B. Kaiser, Dr. J.-F. Bézar, Dr. N. Boudet, Dr. N. Blanc, Dr. S. Kohara, and Dr. H. Tajiri. This work was partially supported by the Japan Society for the Promotion of Science (JSPS) Grant-in-Aid for Scientific Research on Innovative Areas ‘3D Active-Site Science’ (Nos. 26105006 and 15K21719). JRS acknowledges the financial support as Overseas researcher under the Postdoctoral Fellowship of JSPS (No. P16796).

References

- 1) This article is the English interpretation of Bulletin of the Ceramic Society of Japan **52**, 341 (2017).
- 2) J. E. Enderby, D. M. North, and P. A. Egelstaff, *Philos. Mag.* **14**, 961 (1966).
- 3) Y. Waseda, *Novel Application of Anomalous (Resonance) X-Ray Scattering for Structural Characterization of Disordered Materials* (Springer, Berlin, 1984).
- 4) S. Hosokawa, W.-C. Pilgrim, J.-F. Bézar, and S. Kohara, *Eur. Phys. J. Special Topics* **208**, 291 (2012).
- 5) S. Hosokawa, J. R. Stellhorn, W.-C. Pilgrim, and J.-F. Bézar, *Z. Phys. Chem.* **230**, 313 (2016).
- 6) S. Hosokawa, W.-C. Pilgrim, A. Höhle, D. Szubrin, N. Boudet, J.-F. Bézar, and K. Maruyama, *J. Appl. Phys.* **111**, 083517 (2012).
- 7) J. R. Stellhorn, PhD Thesis (Philipps-Univ. Marburg, 2016).
- 8) J. R. Stellhorn, W.-C. Pilgrim, B. Kaiser, N. Boudet, N. Blanc, H. Tajiri, S. Kohara, K.

- Kimura, and S. Hosokawa, Phys. Rev. B, submitted.
- 9) S. Hosokawa and J.-F. Béjar, AIP Conf. Proc. **879**, 1743 (2007).
 - 10) R. L. McGreevy and L. Pusztai, Mol. Simulat. **1**, 359 (1988).
 - 11) N. Metropolis, A. W. Rosenbluth, M. N. Rosenbluth, A. H. Teller, and E. Teller, J. Phys. Chem. **21**, 1087 (1953).
 - 12) O. Gereben, P. Jóvári, L. Temleitner, and L. Pusztai, J. Optoelectron. Adv. Mater. **9**, 3021 (2007).
 - 13) N. Yamada, E. Ohno, K. Nishiuchi, N. Akahira, and M. Takao, J. Appl. Phys. **69**, 2849 (1991).